ScanSAR-Stripmap interferometry using Envisat ASAR data

LIANG Cunren, ZENG Qiming, CUI Xiai, JIAO Jian

Institute of Remote Sensing and GIS, *Peking University*, *Beijing* 100871, *China*

Abstract: This study analyzes the main phase contributions of ScanSAR-Stripmap interferometry and further points out the special component caused by unsynchronized echoes, which is then verified in the experiment. The whole process of ScanSAR-Stripmap interferometry has been proposed and implemented with the help of relating modules of the Repeat Orbit Interferometry Package (ROI_PAC) developed by Jet Propulsion Laboratory (JPL). Coregistration and improvement of coherence are solved emphatically. Finally, ScanSAR-Stripmap interferometry is realized using Envisat ASAR data and the results are compared with those of traditional Stripmap-Stripmap interferometry for validation.

Key words: InSAR, interferometry, ScanSAR, stripmap, burst, synchronized

CLC number: TP722.6 **Document code**: A

Citation format: Liang C R, Zeng Q M, Cui X A and Jiao J. 2011. ScanSAR-Stripmap interferometry using Envisat ASAR data. *Journal of Remote Sensing,* **15**(4): 696–708

1 INTRODUCTION

ScanSAR is a special operation mode of SAR which can greatly extend the overall swath width by cyclically scanning several subswaths, compared with the conventional stripmap mode. However, it was not until the launch of SIR-C in 1994 that ScanSAR has been in operation. The remarkable potential of ScanSAR has been shown in the Shuttle Radar Topography Mission (SRTM) which has mapped the global DEM in only 11 days (JPL, 2000). Most of the recently launched spaceborne SAR instruments can operate in ScanSAR mode with considerable amount of acquisitions. ScanSAR interferometry, which has been preliminarily realized by a Chinese researcher (Jia, 2009), is different from the traditional stripmap interferometry because of its distinct signal characteristics and operation mode. Further more, interferometry using both ScanSAR and stripmap data which is the so called ScanSAR-Stripmap interferometry, is somewhat more difficult. No successful attempt of ScanSAR-Stripmap interferometry by Chinese researcher has been found, despite several examples abroad (Bamler, *et al.*, 1999; Guarnieri & Pasquali, 2003; Guarnieri, *et al.*, 2003; Guccione, 2006; Ortiz & Zebker, 2007). However, ScanSAR-Stripmap interferometry breaks the limit of single mode interferometry and therefore is meaningful. Suppose that there are 4 acquisitions comprised of 2 stripmap ones and 2 ScanSAR ones. If only single mode interferometry (Stripmap-Stripmap, ScanSAR-ScanSAR) is available, then we only have two choices. But if ScanSAR-Stripmap interferometry is possible, there will be 6 choices totally. The more the acquisitions we have, the more additional choices there will be. Therefore, ScanSAR-Stripmap interferometry will highly increase the number of the available interferometric combianations for current SAR dataset archives. It will be of great importance for disaster monitoring. For example, we can only get stripmap data before the earthquake, while the post earthquake data is ScanSAR data. It is obvious that we can not get the deformation caused by the earthquake only using single mode interferometry. However, ScanSAR-Stripmap interferometry can make up for the pity.

The Envisat ASAR instrument launched in 2002 can operate in 5 modes, among which the Wide Swath (WS) and the Global Monitoring (GM) mode are ScanSAR mode. In this paper, we use Envisat ASAR WS and IM (Image mode, stripmap mode) data to study ScanSAR-Stripmap interferometry and show the results.

2 OPERATION MODE AND SIGNAL CHARACTERISTICS OF SCANSAR

In conventional stripmap mode, SAR transmits and receives the pulse of a single beam with a constant pulse repetition frequency (PRF) to image the Earth. ScanSAR, however, scans several subswaths by cyclically switching its antenna elevation angle in order to greatly extend the range width. For a single subswath, ScanSAR operates almost in the same way as stripmap mode, except that ScanSAR transmits pulse sequences with cyclical intervals in which SAR collects echoes of the other subswaths. The pulse sequence is called burst. The bursts and their gaps constitute a subswath. We

Received: 2009-10-16; **Accepted:** 2010-10-22

Foundation: National High Technology Research and Development Program (“863” Program)(No. 2009AA12Z1464;No.2006AA12Z150); ESA-MOST Dragon 2 Cooperation Program (ID: 5343)

First author biography: LIANG Cunren (1986—), male, master candidate of Peking University. His main research interest is about the interferometric processing of synthetic aperture radar data. E-mail: lcriah@163.com

Corresponding author: ZENG Qiming(1964—), male, Ph.D., professor of Peking University. His research interest is microwave remote sensing. E-mail: qmzeng@pku.edu.cn

take ScanSAR mode composed of 2 subswaths as an example as shown in Fig. 1. At location A, SAR transmits and receives pulse sequence (a burst) of subswath 1. When it arrives at location B, it switches its antenna elevation angle to collect echoes (a burst) of subswath 2. Then it switches back to subswath 1 again. The above steps are repeated continuously to complete an acquisition. In this way, ScanSAR can achieve very large range width. However, the azimuth resolution is greatly reduced.

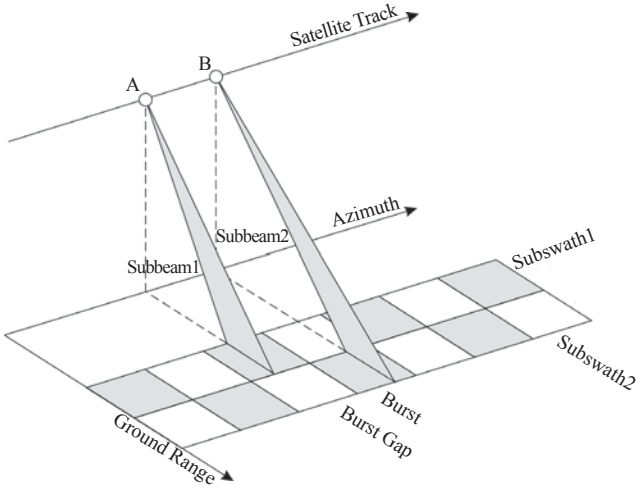

Fig. 1 Operation mode of ScanSAR

Based on the analysis of ScanSAR operation, the azimuth signal of a subswath is shown in Fig. 2. As we can see from this figure, the azimuth (slow time) signal is different from that of stripmap mode. That is, the azimuth is spaced by cyclical gaps which do not exist in stripmap mode. In range direction, however, there is not anything different from stripmap mode.

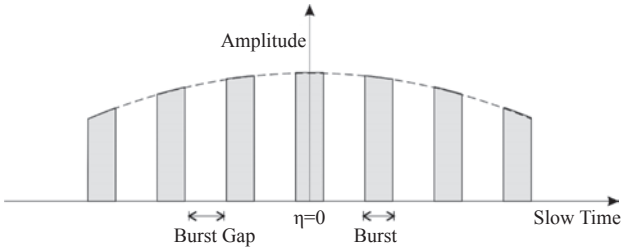

Fig. 2 Azimuth signal of a ScanSAR subswath

To solve the conflict between range resolution and pulse length, the signal transmitted by SAR is linear frequency-modulated (FM). The received signal contains the radar carrier which is removed before the sampling by a quadrature demodulation process. After that, the signal from a single point target can be represented by the complex signal (Cumming & Wong, 2005)

$$s_0(\tau,\eta)=A_0\,w_r(\tau-2R(\eta)/c)w_a(\eta-\eta_c)\times \exp\{-j4\pi R(\eta)/\lambda\}\exp\{j\pi K_r(\tau-2R(\eta)/c)^2\} \quad (1)$$

where τ and η are fast and slow time, respectively.

The received echoes are then focused in order to be adapted to interferometry. Take range Doppler algorithm (RDA) as an example, after the so-called range compression, range cell migration correction (RCMC) and azimuth compression, the single look complex (SLC) can be expressed as

$$s_{\text{stripmap}}(\tau,\eta)=A_0p_r(\tau-2R_0/c)p_a(\eta)\times \exp\{-j4\pi R_0/\lambda\}\exp\{j2\pi f_{c1}\eta\} \quad (2)$$

For ScanSAR, considering the burst gaps, the received signal of a subswath is

$$s_0'(\tau,\eta)=A_0w_r(\tau-2R(\eta)/c)w_a(\eta-\eta_c)w_B(\eta)\times \exp\{-j4\pi R(\eta)/\lambda\}\exp\{j\pi K_r(\tau-2R(\eta)/c)^2\} \quad (3)$$

As we can see from Eq. (3), comparing with Eq. (1), the received signal of ScanSAR can be taken as stripmap signal imposed with a window $w_B(\eta)$, which is also what Fig. 2 tries to depict.

There already exist many algorithms which can be used to focus Eq. (3) such as full-aperture algorithm, the modified SPECAN algorithm and the ECS algorithm. To make full use of the availability of the existing resources, full aperture algorithm is adopted to focus the raw data, which can keep all the phase information we need. It requires that the burst gaps should be padded with zeros. Then the zero-padded signal can be put into the conventional focusing algorithm and the resultant SLC can be expressed as

$$s_{\text{ScanSAR}}(\tau,\eta)\approx A_0B_BB_pB_ap_r(\tau-2R_0/c)\times \exp\{-j4\pi R_0/\lambda\}\text{sinc}(B_B\eta)III(B_p\eta)\times \exp\{-j2\pi K_a\eta_{\text{shift}}\eta\}\exp\{j2\pi f_c\eta\} \quad (4)$$

3 THEORETICAL BASIS OF SCANSAR-STRIPMAP INTERFEROMETRY

Suppose that the master image is stripmap mode data, while the slave is ScanSAR mode data. Then the slave image can be described as

$$s_{\text{ScanSAR}}(\tau,\eta)\approx A_0B_BB_pB_ap_r(\tau-2(R_0+\Delta R)/c)\times \exp\{-j4\pi(R_0+\Delta R)/\lambda\}\times \text{sinc}(B_B\eta)III(B_p\eta)\exp\{-j2\pi K_a\eta_{\text{shift}}\eta\}\times \exp\{j2\pi f_{c2}\eta\} \quad (5)$$

After coregistration, it is written as

$$s_{\text{ScanSAR}}'(\tau,\eta)\approx A_0B_BB_pB_ap_r(\tau-2R_0/c)\times \exp\{-j4\pi(R_0+\Delta R)/\lambda\}\times \text{sinc}(B_B\eta)III(B_p\eta)\times \exp\{-j2\pi K_a\eta_{\text{shift}}\eta\}\exp\{j2\pi f_{c2}\eta\} \quad (6)$$

The interferogram is

$$Interferogram(\tau,\eta)=s_{\text{stripmap}}\times s'^{*}_{\text{ScanSAR}} \quad (7)$$

The phase of the interferogram is composed of the following three components

$$\exp\{j4\pi\Delta R/\lambda\} \quad (8)$$

$$\exp\{j2\pi(f_{c1}-f_{c2})\eta\} \quad (9)$$

$$\exp\{-j2\pi K_a\eta_{\text{shift}}\eta\} \quad (10)$$

where η_{shift} is the time shift between the burst center and the zero Doppler centroid, K_a is the azimuth FM rate, η is slow time. Eq. (8) and Eq. (9), which also exist in stripmap interferometry, are caused by the topography and the difference between the Doppler centroid of the interferometric pair, respectively. Eq. (10) is caused by the pattern of acquiring data in ScanSAR mode. It contaminates the interferometric phase and reduces the coherence of the interferometric pair. It is the key problem that will be dealt with in this paper.

There are two solutions for Eq. (10), one of which is to filter the stripmap data by a low-pass filter (Guccione, 2006). The other one is to remove some of the echoes of stripmap mode, according to the burst gaps of ScanSAR mode. Therefore, the resultant SLC of stripmap mode will also have phase like Eq. (10), which will be removed automatically in interferometry along with phase Eq. (10)

in ScanSAR mode. The latter approach is chosen as our processing strategy to implement ScanSAR-Stripmap interferometry.

4 KEY TECHNOLOGIES OF SCANSAR-STRIPMAP INTERFEROMETRY

In order to realize ScanSAR-Stripmap interferometry, we have modified the ROI_PAC (Repeat Orbit Interferometry Package) (Rosen, *et al.*, 2004) software developed by Jet Propulsion Laboratory.

ROI_PAC is a repeat orbit interferometric package. The source code of ROI_PAC has been freely available to the InSAR community since 2000. Current version of ROI_PAC is V3.0.1. ROI_PAC implements its fundamental algorithms in C and Fortran 90 and drives each executable module with a Perl control script, running on SGI, Sun, Mac OS X, and Linux platforms (Rosen & Fielding, 2009). It is designed to only implement stripmap interferometry.

Based on ROI_PAC, the ScanSAR-Stripmap interferometry we proposed includes the following key technologies: (1) Unification of the PRF of the two datasets. (2) Coregistration. (3) Removal of the unsynchronized echoes. (4) Extraction of the overlapped area.

4.1 Unification of the PRF of the two datasets

The interferometric processing requires that the interferometric pair shares the same PRF and range resampling frequency. Although the two datasets are in the same swath, they have different PRF. Therefore, one of the datasets should be resampled in azimuth. Considering the higher PRF of ScanSAR, the stripmap data is resampled in order to keep in accordance with ScanSAR.

A phase-preserving interpolation kernel should be used in resampling because interferometry requires keeping phase information. We use *sinc* function because of its excellent performance. However, the length of *sinc* kernel is infinite, indicating that we have to adopt a truncated *sinc* kernel. In implementation, we use a 16-point *sinc* kernel since improvement is marginal when a kernel length longer than 16 points is used (Cumming & Wong, 2005). On the other hand, the increase in the length of kernel will also lead to additional calculation.

4.2 Coregistration

Although correlation is used to coregister slave image to master image in ROI_PAC, we found that it did not work well for ScanSAR-Stripmap interferometry. Therefore, we propose the method of three-time iteration coregistration based on the conventional coregistration strategy.

First, we use satellite ephemeris to calculate the azimuth offset that will be the basis of removing the unsynchronized echoes. The slave image is then coregistered to the master image according to the azimuth offset. Echoes corresponding to the burst gaps of ScanSAR are replaced with zeros. This manipulation can roughly keep the synchronization of the two datasets and therefore will improve the coherence of the interferometric pair. In addition, the azimuth resolution of stripmap data will be the same as that of ScanSAR, as well as some other signal characteristics. In a word, the precision of this azimuth offset can actually meet the need of coregistration in this step.

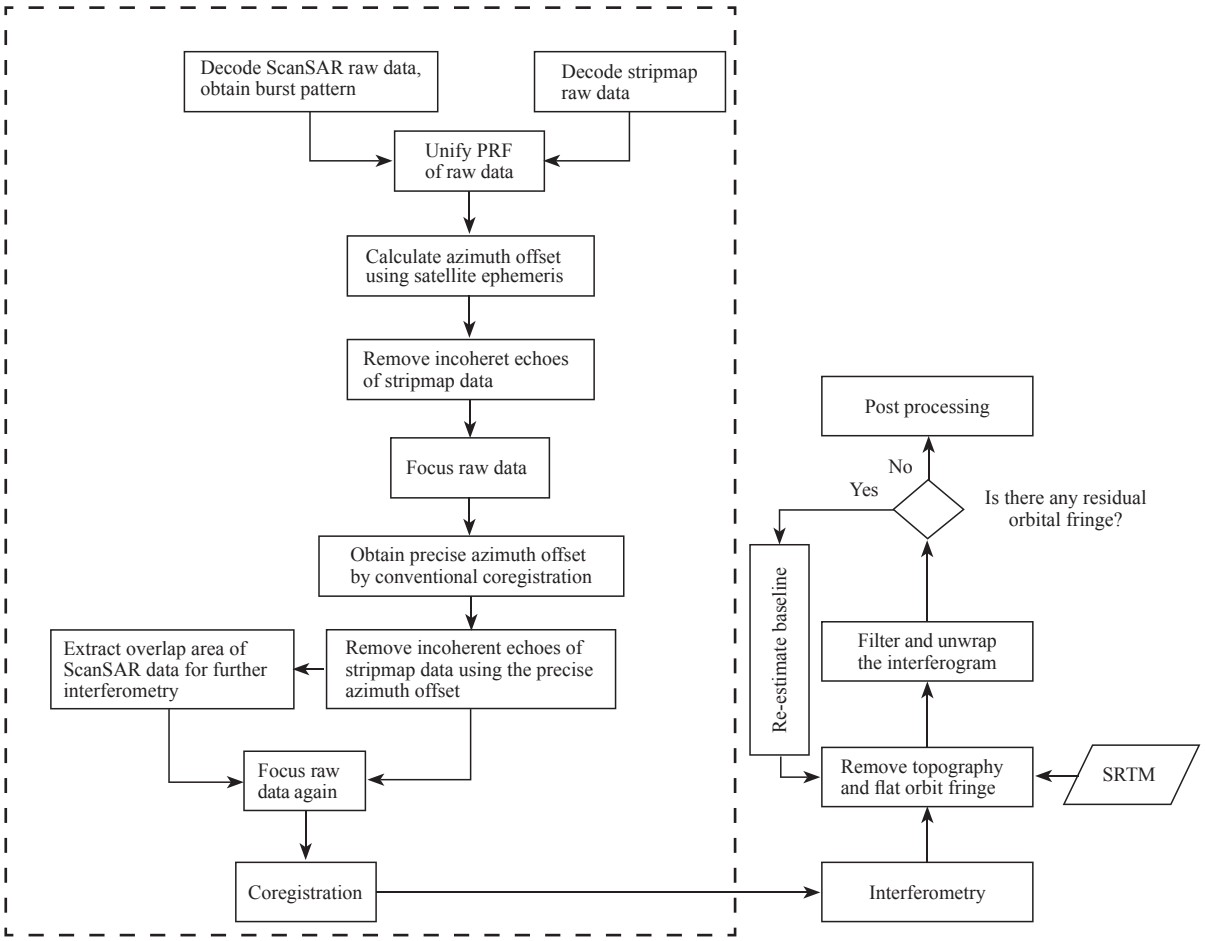

Fig. 3 Flow chart of ScanSAR-Stripmap differential interferometry

The ScanSAR and resultant stripmap raw data is then focused and coregistered using the correlation method. In this step, we will get a better azimuth offset which is used to replace the unsynchronized echoes of stripmap data in the same way as above mentioned method. Finally, the newly processed stripmap raw data is focused and coregistered again. After that, the coregistration is completed.

4.3 Removal of the unsynchronized echoes

In section 3, we have demonstrated that the effect of Eq. (10) should be properly removed in ScanSAR-Stripmap interferometry. Therefore, if the line in stripmap data is zero-line or echo-line, the corresponding line in ScanSAR data should be the same, which is also called synchronization. Otherwise, the coherence of the interferometric pair will be reduced and the interferogram will be contaminated by the needless phase. However, there is no need to seek very precise synchronization. Actually, we have properly removed the unsynchronized echoes of stripmap data in the second step of coregistration described in section 4.2, meaning that the synchronization of the interferometric pair is assured.

4.4 Extraction of the overlap area

In order to save computation load and improve the precision of the processing, only the overlap area of the interferometric pair is extracted for further processing. Actually, the area in ScanSAR data corresponding to the stripmap data is extracted because of its much larger coverage.

The key processing flow is summarized in the dashed line frame of Fig. 3. After that, the results can be applied to DEM generation or surface displacement detection.

5 SCANSAR-STRIPMAP INTERFEROMETRY EXPERIMENT AND ITS ANALYSIS

There are two experiments in this study: (1) Verification of the effect of Eq. (10) on coherence. (2) ScanSAR-Stripmap interferometry. We choose the Envisat ASAR WS (ScanSAR) and IM (Stripmap) data of Bam, Iran earthquake provided by the ESA-MOST Dragon Programme as the experimental data which is shown in Table 1.

Table 1 Experimental data

Interferometric Combination		Date	Track
ScanSAR-Stripmap	Master	2003-09-24	120
	Slave	2004-02-11	120
Stripmap-Stripmap	Master	2003-12-03	120
	Slave	2004-02-11	120

5.1 Verification of the effect of Eq. (10) on coherence

Two schemes are proposed to verify the effect of Eq. (10) on coherence. In scheme 1, the stripmap data without incoherent echoes removal is used for interferometry, while the stripmap data with incoherent echoes removal is used in scheme 2. A 5×5 window is employed to calculate the interferometric coherence. The coherence maps in the two schemes are shown in Fig. 4 which indicates that the coherence of the interferometric pair is highly improved after incoherent echoes removal. The mean coherence of scheme 2 is 0.49, 2.2 times of that in scheme 1, whose mean coherence is 2.2. Now the effect of (10) is clearly verified.

5.2 ScanSAR-Stripmap interferometry

The key technologies proposed in section 4 are applied to the repeat orbit differential interferometry. The overall processing flow is shown in Fig. 3. The results are compared with those of conventional stripmap interferometry (Stripmap-Stripmap).

The coherence map of ScanSAR-Stripmap interferometry is shown in Fig. 4 (b). Compared to the coherence of stripmap-stripmap interferometry shown in Fig. 4 (c), it is a little bit lower. The mean coherence of Fig. 4 (b) and (c) is 0.49 and 0.69, respectively. This is reasonable with following speculations. First, the time span of the ScanSAR-Stripmap interferometric pair is longer, during which there may be climatic and seasonal factors that reduce coherence. Second, errors of synchronization will affect the coher-

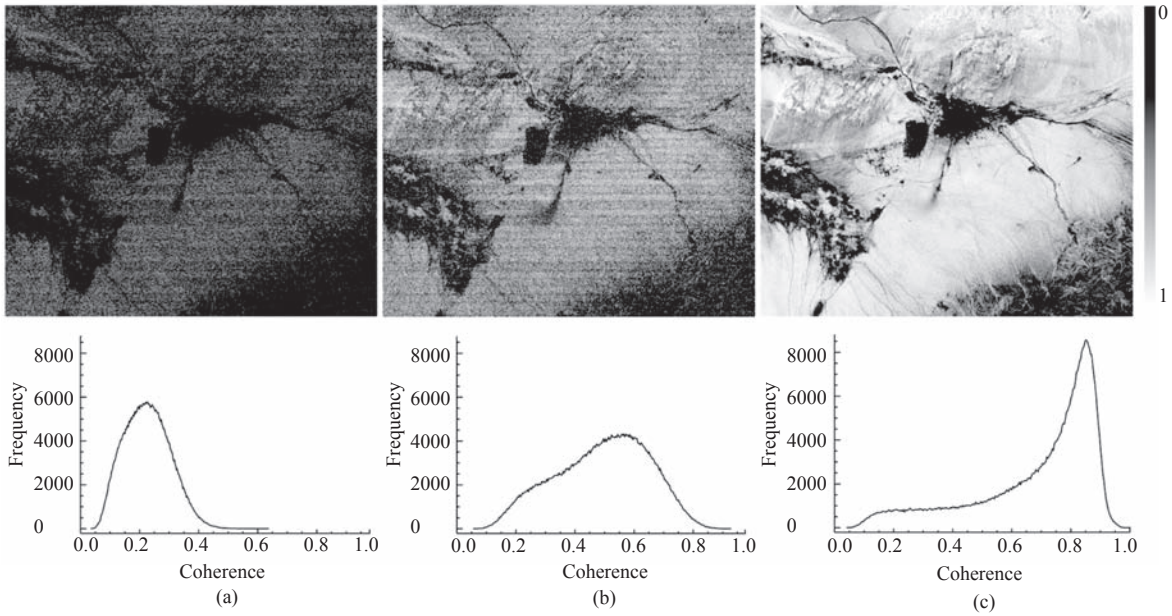

Fig. 4 Coherence maps and their histograms.
(a) Coherence map of ScanSAR-Stripmap interferometry without incoherent echoes removal; (b) Coherence map of ScanSAR-Stripmap interferometry with incoherent echoes removal; (c) Coherence map of Stripmap-Stripmap interferometry

ence of ScanSAR-Stripmap interferometry. Third, the much coarser azimuth resolution of ScanSAR-Stripmap interferometry may also be the cause of low coherence. In addition, different systematic parameters used in the acquisitions of the two modes may be another factor that affects coherence.

The differential interferograms of ScanSAR-Stripmap and Stripmap-Stripmap interferometry are shown in Fig. 5 (a) and (b). Generally, they both show a similar pattern. The interferometric results need further quantitative comparison which is illustrated in Fig. 6. The maximum and minimum LOS deformations of ScanSAR-Stripmap interferometry are 30.7 cm and – 17.4 cm. The values of Stripmap-Stripmap interferometry are 30.5 cm and – 17.3 cm. Local difference between Fig. 6 (a) and (b) in the lower left corner is caused by the masking of pixels with low coherence in (a). The result of Stripmap-Stripmap interferometry shown in Fig. 6 (b) can be treated as the real deformation. Then the fact that Fig. 6 (a) and (b) are in good agreement which suggests that the method proposed in this paper is workable.

Additionally, the low azimuth resolution of ScanSAR together with the low PRF of stripmap mode in this experiment leads to a resolution of ScanSAR-Stripmap interferometry even coarser than that of ScanSAR interferometry.

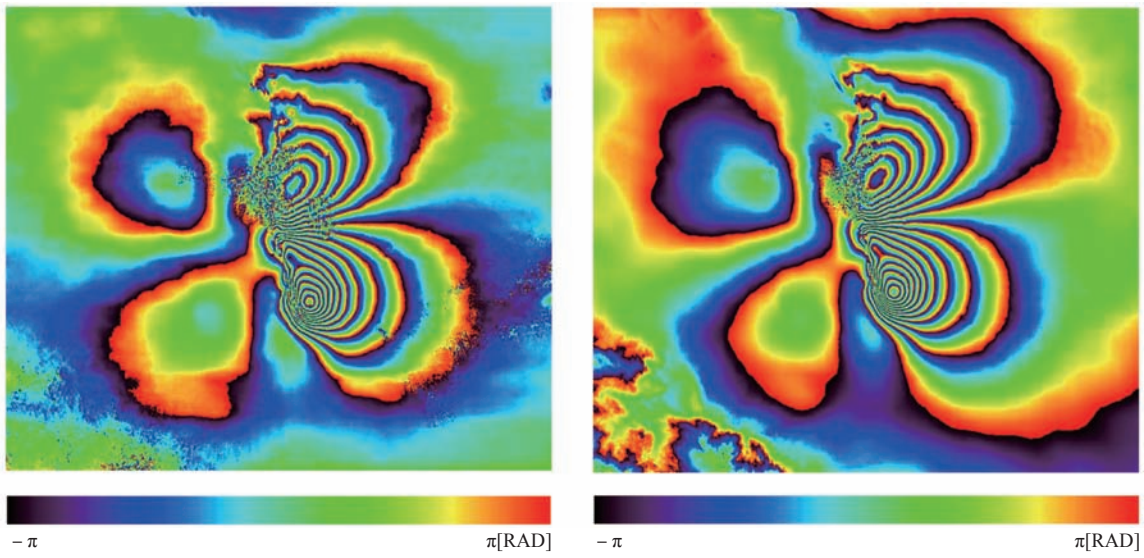

Fig. 5 Comparison of ScanSAR-Stripmap and Stripmap-Stripmap differential interferograms (wrapped phase)
(a) ScanSAR-Stripmap; (b) Stripmap-Stripmap

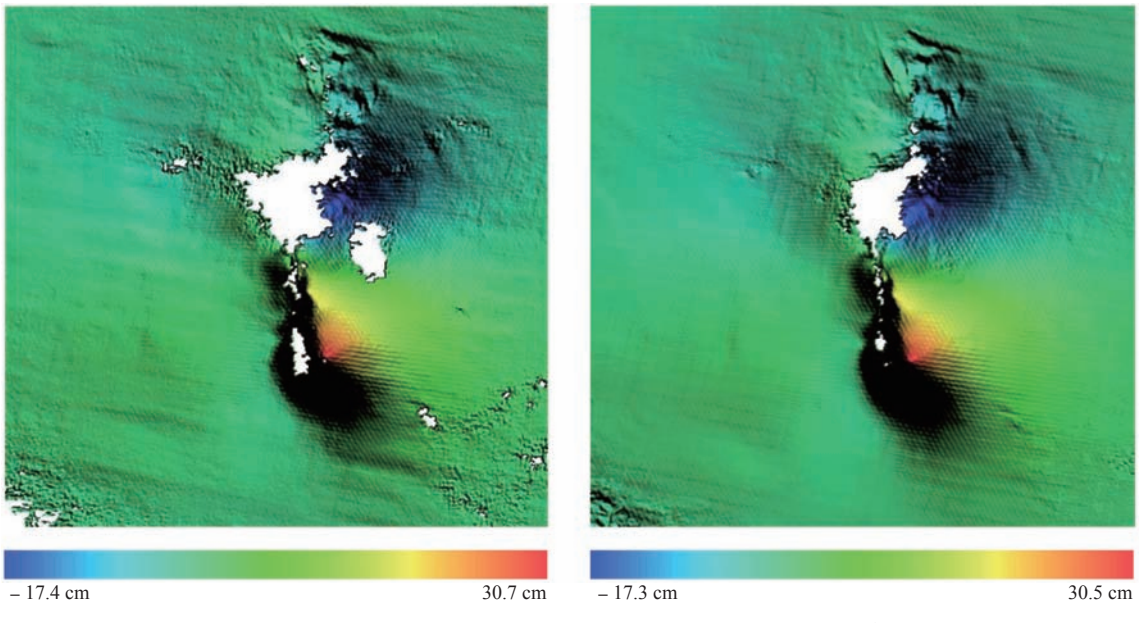

Fig. 6 Comparison of 3D surface view of displacement maps derived by ScanSAR-Stripmap and Stripmap-Stripmap differential interferometry (White pixels are invalid because of low coherence)
(a) ScanSAR-Stripmap; (b) Stripmap-Stripmap

6 CONCLUSION

First, we have proposed some key technologies based ROI_PAC which are then adapted to ScanSAR-Stripmap interferometry, including unification of the PRF of the two datasets, coregistration, removal of the unsynchronized echoes and so on. These technologies are applied to the differential interferometry of Iran, Bam earthquake using Envisat ASAR data. Comparison of the results of ScanSAR-Stripmap and Stripmap-Stripmap interferometry shows that they are in good agreement with each other, suggesting that the method proposed in this paper is reliable.

Second, we have analyzed the main phase contributions of ScanSAR-Stripmap interferometry and further points out the special component that is verified with an experiment.

Third, we have developed a set of programs for ScanSAR-Stripmap interferometry based on ROI_PAC.

Acknowledgements: We thank JPL for its freely available open source interferometric package ROI_PAC.

REFERENCES

Bamler R, Geudtner D, Schattler B, Vachon P W, Steinbrecher U, Holzner J, Mittermayer J, Breit H and Moreira A. 1999. RADARSAT ScanSAR interferometry. IEEE International Geoscience and Remote Sensing Symposium Proceedings. Piscataway: Institute of Electrical and Electronics Engineers, Inc: 1517–1521

Cumming I G and Wong F H. 2005. Digital Processing of Synthetic Aperture Radar Data: Algorithms and Implementation. Norwood, MA: Artech House, Inc: 57–58, 144

Guarnieri A M, Cafforio C, Guccione P, Pasquali P and Desnos Y L. 2003a. ENVISAT ASAR ScanSAR interferometry. IEEE International Geoscience and Remote Sensing Symposium Proceedings. Piscataway: Institute of Electrical and Electronics Engineers, Inc: 1124–1126

Guarnieri A M, Guccione P, Pasquali P and Desnos Y L. 2003b. Multi-mode ENVISAT ASAR interferometry: techniques and preliminary results. *IEE Proceedings-Radar*, *Sonar and Navigation*, **150**(3): 193–200

Guccione P. 2006. Interferometry with ENVISAT wide swath ScanSAR data. *IEEE Geoscience and Remote Sensing Letters*, **3**(3): 377–381

Jia J Y. 2009. ScanSAR Interferometry Processing Techni-Que and Experiments. Beijing: Peking University: 79–80

JPL. [2009-09-17]. http://www2. jpl. nasa. gov/srtm/

Ortiz A B and Zebker H. 2007. ScanSAR-to-stripmap mode interferometry processing using ENVISAT/ASAR data. *IEEE Transactions on Geoscience and Remote Sensing*, **45**(11): 3468–3480

Rosen P A and Fielding E. 2009. ROI_PAC. OPEN CHANNEL FOUNDATION. [2009-09-18]. http: //www.openchannel software.com/projects/ROI_PAC

Rosen P A, Henley S, Peltzer G and Simons M. 2004. Updated repeat orbit interferometry package released. *EOS*, *Transactions American Geophysical Union*, **85**(5): 47

Envisat ASAR ScanSAR-Stripmap 干涉测量研究

梁存任，曾琪明，崔喜爱，焦健

北京大学 遥感与地理信息系统研究所，北京 100871

摘 要：分析了ScanSAR-Stripmap干涉测量的相位组成，指出其因非同步数据引起的特有相位项，并通过实验验证了该相位项的存在。提出一整套ScanSAR-Stripmap干涉测量方法，借助JPL开发的开源干涉测量软件ROI_PAC的相应模块实现干涉处理过程，重点解决了ScanSAR-Stripmap两种模式数据间的配准以及相干性的提高等问题。用Envisat ASAR数据验证了该方法的可行性。最后将实验结果同常规条带式干涉测量结果做了对比与分析，验证了该方法的正确性。

关键词：合成孔径雷达，干涉测量，ScanSAR，条带模式，片段，同步

中图分类号：TP722.6 **文献标志码**：A

引用格式：梁存任，曾琪明，崔喜爱，焦健. 2011. Envisat ASAR ScanSAR-Stripmap 干涉测量研究. 遥感学报，**15**(4)：696–708
Liang C R, Zeng Q M, Cui X A and Jiao J. 2011. ScanSAR-Stripmap interferometry using Envisat ASAR data. *Journal of Remote Sensing*, **15**(4): 696–708

1 引 言

扫描模式SAR(Scanning Synthetic Aperture Radar, ScanSAR)可以大幅增加距离向的测绘带宽，从而实现大面积观测。但是早期SAR系统的工作模式都是条带(Stripmap)模式，直到1994年的SIR-C才真正实现了ScanSAR工作模式。2000年美国航天飞机雷达地形测绘任务SRTM在11天之内获取了全球的DEM显示了ScanSAR的巨大优势(JPL，2000)。近年来发射的一些星载SAR都具备ScanSAR模式数据获取能力，而且ScanSAR数据在SAR获取的数据中占有相当大的比重。由于ScanSAR独特的工作模式和信号特点，ScanSAR干涉测量有许多方面不同于常规条带式干涉测量，国内已经有研究者(贾建瑛，2009)实现了该种干涉测量。而将ScanSAR数据和条带模式数据进行混合干涉测量在技术上更增加了难度，国内尚没有这方面的研究，少数国外学者对其做了研究(Bamler 等，1999；Guarnieri 等，2003a，2003b；Guccione，2006；Ortiz和Zebker，2007)。但是这种干涉处理方式拓宽了干涉测量范围，使干涉测量不再局限于单模式数据间的干涉，具有重要意义。设想有4景数据：两景条带式数据，两景ScanSAR数据，假如只进行同种模式数据间(Stripmap-Stripmap、ScanSAR-ScanSAR)的干涉测量，那么只有两种选择；如果再进行ScanSAR和条带模式数据间(ScanSAR-Stripmap)的干涉测量，可以将可能的选择提高到6种。随着数据的增多，增加的选择会更多。可见ScanSAR-Stripmap干涉可以大大提高现有数据的利用率。特别是对于一些突发性事件的监测具有重要意义，如地震前只有条带模式数据，地震后只有ScanSAR数据，显然同种模式干涉测量对于地表形变监测显得无能无力，而ScanSAR-Stripmap干涉测量可以弥补缺憾。

2002年欧空局发射的Envisat卫星搭载的合成孔径雷达ASAR具有多种工作模式，其Wide Swath (WS)、Global Monitoring (GM)等模式都属于ScanSAR模式。本研究利用Envisat ASAR WS(ScanSAR)和IM(Stripmap)模式数据对ScanSAR-Stripmap干涉测量进行了探索性研究，并取得了理想的实验结果。

收稿日期：2009-10-16；**修订日期**：2010-10-22

基金项目：国家高技术研究发展计划(863计划)(编号：2009AA12Z1464；编号：2006AA12Z150)；中国科技部—欧洲空间局合作“龙计划”二期项目(编号：5343)

第一作者简介：梁存任(1986—)，男，北京大学硕士研究生，目前主要从事SAR干涉处理等方面的研究。E-mail: lcriah@163.com。

通信作者：曾琪明，E-mail: qmzeng@pku.edu.cn。

2 ScanSAR工作模式及信号特点

条带式SAR的工作模式是对同一个条带以相同的脉冲重复频率PRF (Pulse Repetition Frequency)连续地发射与回收信号，实现对地观测。而ScanSAR是通过周期性地调整天线的角度对多个子条带扫描，实现距离向大面积观测。在每一个子条带之内其工作模式与条带式的工作模式大致相同，只是在该子条带之内周期性地以一定时间间隔发射脉冲序列，每一个连续的脉冲序列称为一个片段(burst)，这些周期性的片段连同时间间隔构成了一个子条带，而在时间间隔之内SAR调整天线角度来获取其他子条带的数据。以包含两个子条带的ScanSAR工作模式为例，如图1所示，当SAR在位置A时，SAR调整天线角度向子条带1发射并回收一系列脉冲，构成一个片段。随着遥感平台的飞行，在位置B时，SAR调整天线角度，向子条带2发射并回收脉冲形成子条带2的一个片段，然后再将天线角度调整到指向子条带1。这样不断重复这个过程就实现了ScanSAR数据获取。虽然ScanSAR以这样的数据获取方式实现了大面积观测，但是同时也降低了其方位向分辨率。

基于以上对ScanSAR独特工作模式的分析，ScanSAR单一条带在方位向上的回波信号如图2所示。从图中可以看出，ScanSAR信号与条带模式信号在方位向(图中所示慢时间)上有明显的不同，即在方位向上有周期性的间隔，而条带式数据并没有这个间隔。在距离向上，ScanSAR的回波信号与条带模式并没有差别。

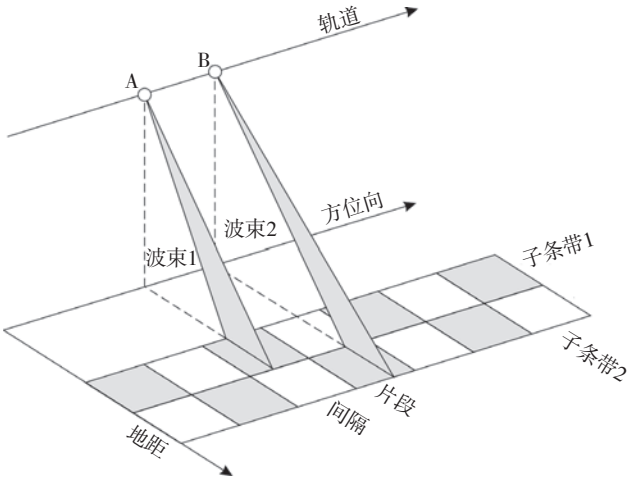

图1 ScanSAR工作模式

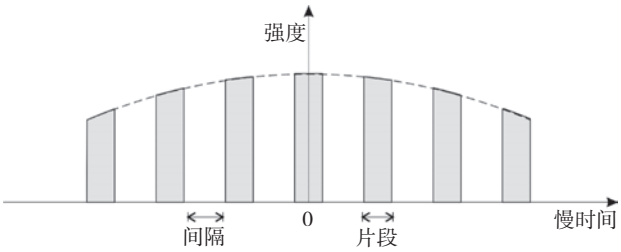

图2 ScanSAR子条带方位向回波信号

下面分析两种模式信号。为了解决距离向分辨率与脉冲宽度的矛盾，目前的SAR系统普遍采用线性调频技术，SAR发射的脉冲信号是一个线性调频实信号，天线接收到的回波信号是解调制去除了高频载波的复信号(Cumming 和 Wong，2005)：

$$s_0(\tau,\eta)=A_0\,w_r(\tau-2R(\eta)/c)w_a(\eta-\eta_c)\times \exp\{-j4\pi R(\eta)/\lambda\}\exp\left\{j\pi K_r(\tau-2R(\eta)/c)^2\right\} \quad (1)$$

式中，τ、η分别是快时间和慢时间。

为了进行干涉处理，需要将原始回波信号处理成单视复数影像(Single Look Complex，SLC)。以距离多普勒算法(RDA)为例，将原始信号依次进行距离向压缩、距离向徙动校正、方位向压缩之后的信号表达式为：

$$s_{\text{stripmap}}(\tau,\eta)=A_0p_r(\tau-2R_0/c)p_a(\eta)\times \exp\{-j4\pi R_0/\lambda\}\exp\{j2\pi f_{c1}\eta\} \quad (2)$$

由于ScanSAR在方位向的间歇扫描特点，单一子条带的ScanSAR信号为：

$$s_0'(\tau,\eta)=A_0w_r(\tau-2R(\eta)/c)w_a(\eta-\eta_c)w_B(\eta)\times \exp\{-j4\pi R(\eta)/\lambda\}\exp\left\{j\pi K_r(\tau-2R(\eta)/c)^2\right\} \quad (3)$$

从公式(3)中可以看出，与条带模式信号(1)相比，ScanSAR信号相当于在方位向对条带模式信号加了窗$w_B(\eta)$，而这也正是图2所描述的特点。

目前已经开发出几种ScanSAR信号成像算法，例如全孔径成像算法、改进的SPECAN算法、ECS算法等。为了充分利用现有条带式SAR成像算法，本研究使用相位保留的全孔径成像算法，其基本做法就是在单个子条带之内将片段之间的时间间隔补零，然后将补零后的子条带数据按照条带式数据成像算法成像。经过全孔径成像算法处理得到的单视复数影像的表达式为：

$$s_{\text{ScanSAR}}(\tau,\eta)\approx A_0B_BB_pB_ap_r(\tau-2R_0/c)\times \exp\{-j4\pi R_0/\lambda\}\text{sinc}(B_B\eta)III(B_P\eta)\times \exp\{-j2\pi K_a\eta_{\text{shift}}\eta\}\exp\{j2\pi f_c\eta\} \quad (4)$$

3 ScanSAR-Stripmap干涉理论基础

假设以条带模式数据作为主影像，以ScanSAR数据作为辅影像。那么辅影像的表达式为：

$$\begin{aligned} s_{\text{ScanSAR}}(\tau,\eta) \approx & A_0 B_B B_p B_a p_r(\tau-2(R_0+\Delta R)/c)\times \\ & \exp\{-j4\pi(R_0+\Delta R)/\lambda\}\times \\ & \text{sinc}(B_B\eta)III(B_P\eta)\exp\{-j2\pi K_a\eta_{\text{shift}}\eta\}\times \\ & \exp\{j2\pi f_{c2}\eta\} \end{aligned} \tag{5}$$

经过配准之后，辅影像表达式为：

$$\begin{aligned} s_{\text{ScanSAR}}'(\tau,\eta) \approx & A_0 B_B B_p B_a p_r(\tau-2R_0/c)\times \\ & \exp\{-j4\pi(R_0+\Delta R)/\lambda\}\times \\ & \text{sinc}(B_B\eta)III(B_P\eta)\times \\ & \exp\{-j2\pi K_a\eta_{\text{shift}}\eta\}\exp\{j2\pi f_{c2}\eta\} \end{aligned} \tag{6}$$

干涉图即：

$$Interferogram(\tau,\eta) = s_{\text{stripmap}} \times s^{*}_{\text{ScanSAR}} \tag{7}$$

这样得到的干涉图中有三项相位，分别是：

$$\exp\{j4\pi\Delta R/\lambda\} \tag{8}$$

$$\exp\{j2\pi(f_{c1}-f_{c2})\eta\} \tag{9}$$

$$\exp\{-j2\pi K_a\eta_{\text{shift}}\eta\} \tag{10}$$

式中，η_{shift}是片段中心相对于零多普勒时刻的时间，K_a是方位向调频率，η是慢时间。其中，式(8)(9)项分别是由于地形以及主辅影像多普勒中心差异造成的，与条带模式数据间的干涉相同。而式(10)项则是由于ScanSAR数据的独特获取方式造成的，这一项会降低数据的相干性，在干涉图中表现为噪声，这是两种模式数据进行干涉处理的关键项。

要消除式(10)项相位的影响，有两种方法可供选择，一种是对条带式数据做低通滤波(Guccione，2006)；另一种是将条带式数据人为地处理成ScanSAR数据(实际上仅是ScanSAR的一个子条带)，即将相应的数据行替换成零，这样也会产生ScanSAR数据所特有的相位项，从而在进行干涉处理时达到抵消多余相位，去掉式(10)的目的。显然第二种方法比第一种方法简单，因此本研究采用第二种方法作为实现ScanSAR-Stripmap干涉的核心思想。

4 ScanSAR-Stripmap干涉关键技术

为进行ScanSAR-Stripmap干涉测量，我们对美国喷气推进实验室(Jet Propulsion Laboratory，JPL)开发的ROI_PAC(Rosen 等，2004)软件(Repeat Orbit Interferometry Package)进行了二次开发。

ROI_PAC是一款开源的重复轨道干涉测量软件，其源代码自2000年开放以来，目前已发展到V3.0.1版。软件底层功能模块由C和Fortran程序编写，软件用Perl脚本程序调用底层功能模块完成相应的干涉处理过程。ROI_PAC可运行于Linux、SGI和Sun等平台下(Rosen和Fielding，2009)，仅支持条带式数据的干涉处理。

基于ROI_PAC，本研究提出的ScanSAR-Stripmap干涉测量方法主要包括以下关键技术：(1)两种模式数据PRF的统一；(2)两种模式数据的配准；(3)不同步数据的去除；(4)相同覆盖原始数据的截取。

4.1 两种模式数据PRF的统一

干涉处理要求两景影像的PRF和距离向采样频率必须相同。在同一个条带，Envisat ASAR两种模式数据的PRF还是不同，需要利用插值函数将一种模式数据的PRF统一到另一种模式数据的PRF上。由于ScanSAR数据的PRF高于条带式数据，实验中对条带式原始信号做了插值，使其PRF与ScanSAR数据对应条带的PRF相同。

干涉测量要求数据处理过程保留相位信息，因此应该使用相位保留的插值核。鉴于*sinc*函数的优良特性，研究中采用*sinc*函数对条带式原始信号做插值处理。*sinc*函数插值核的长度是无限的，实际中无法做到这一点，事实上，当插值核长度超过16的时候，插值精度提高已经不明显了(Cumming和Wong，2005)，而再提高长度会增加计算量，因此采用长度为16的*sinc*函数插值核。

4.2 两种模式数据的配准

虽然ROI_PAC采用开窗计算相关性的原理对两景影像进行配准，但是实验中发现，直接将两景影像处理成分辨率不同的SLC，然后用普通的配准程序配准还是有一定困难。为此我们提出了 3 次迭代的配准方法。

首先根据轨道数据计算方位向偏移，依据这个方位向偏移将条带式数据处理成ScanSAR数据，方法如下：将两种数据根据方位向偏移量对齐，将条带模式数据对应于ScanSAR数据零数据行的数据行替换成零，其他数据行保持不变。这样可以粗略保证两种数据之间的同步性，提高相干性，同时将两景影像的分辨率调节至大体相同，信号特点也基本相同，实际上

这样的精度对配准来说已经达到要求了。然后将处理好的原始数据成像后按照计算相关性的方法做配准，计算出精确的方位向偏移量，依据这个精确的偏移量将条带式数据用同样方法再次处理成ScanSAR数据，再次进行配准，最终完成配准过程。

4.3 不同步数据的去除

前面已经介绍过，要进行ScanSAR数据同条带式数据的干涉处理，必须去掉式(10)的影响，也就是保证两种模式数据相对应的数据行同为真实数据行或者是补零的数据行，即同步性，否则会降低相干性，干涉图中会出现较多的非同步性带来的噪声。但是同步性并不需要特别高的精度。实际上，4.2迭代配准过程中的第 2 次配准计算出了精确的偏移量，从而在将条带式数据处理成ScanSAR数据时较好地去除了不同步数据。

4.4 相同覆盖原始数据的截取

为了节省计算时间，提高数据处理精度，实验中仅对具有相同覆盖的原始数据做干涉处理。由于ScanSAR数据子条带覆盖的地面面积比较大，所以将ScanSAR数据对应于条带式数据的部分截取出来与条带式数据做干涉处理。

综上，该方法的关键技术流程如图3中的虚线框中所示。经过图3虚线框中的处理之后，结合不同的应用目的可以进行干涉测量获取DEM，或者差分干涉测量监测地表形变。

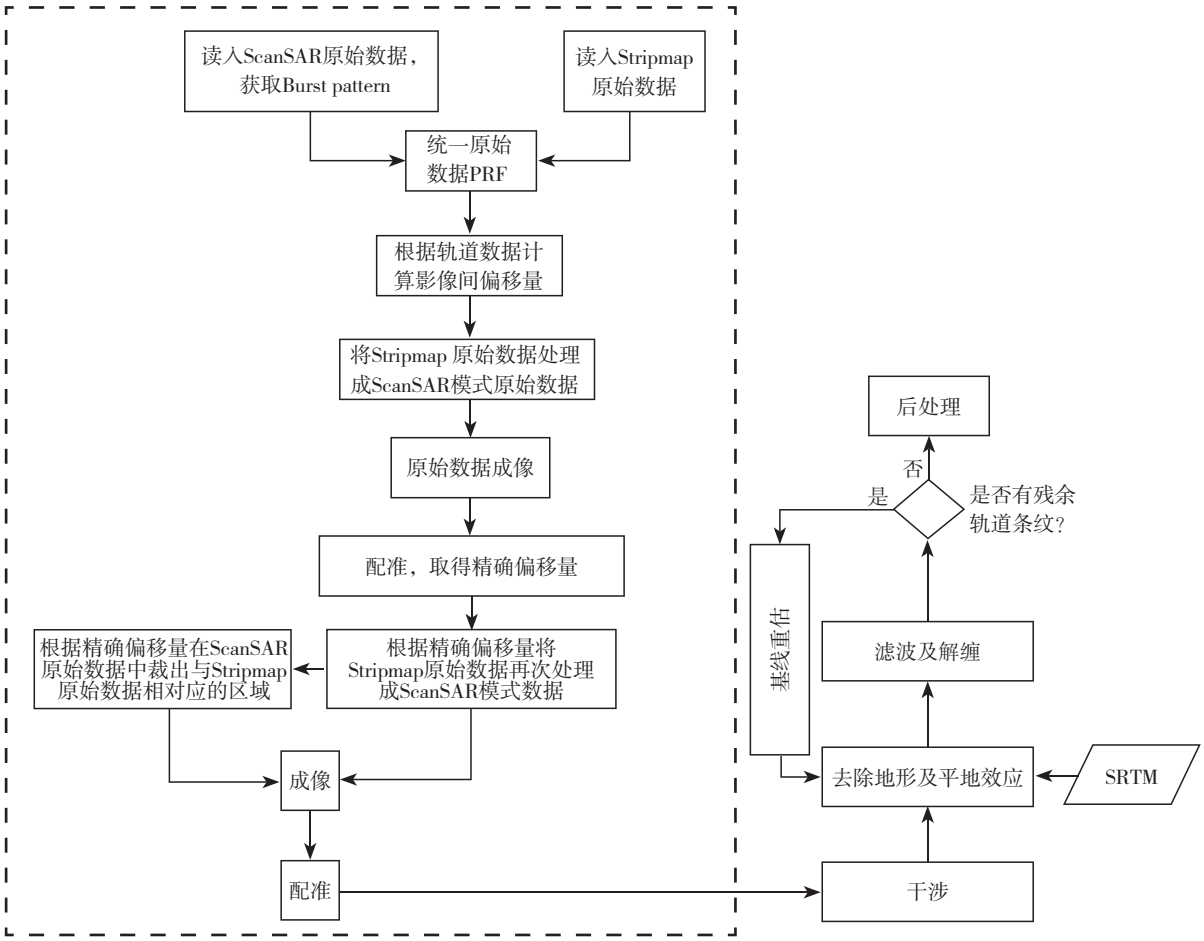

图3 ScanSAR-Stripmap差分干涉测量流程图

5 ScanSAR-Stripmap干涉实验及结果分析

本研究共做了两个实验：(1)式(10)影响相干性的验证；(2)ScanSAR-Stripmap重复轨道差分干涉测量。实验数据选取中欧合作“龙计划”提供的Envisat ASAR WS(ScanSAR)和IM(Stripmap)模式的伊朗巴姆地震数据(表1)。

表1 实验数据

干涉组合		日期	轨道
ScanSAR-Stripmap	主影像	2003-09-24	120
	辅影像	2004-02-11	120
Stripmap-Stripmap	主影像	2003-12-03	120
	辅影像	2004-02-11	120

5.1 式(10)影响相干性的验证

为验证式(10)对相干性的影响，提出两个实验方案，方案1是用条带式数据与ScanSAR数据做干涉处理；方案2是用处理成ScanSAR数据的条带式数据与ScanSAR数据做干涉处理。实验中采用5 × 5的窗口估算干涉相干性。两个实验方案的相干性图及其直方图如图4中(a)、(b)所示。从图中可以看出，将条带式数据处理成ScanSAR数据可以明显提高数据间的相干性。方案1的相干性均值为0.22，方案2的相干性均值为0.49，条带式数据处理成ScanSAR数据之后，与ScanSAR数据的相干性是未经处理成ScanSAR数据时相干性的2.2倍。这就验证了式(10)对相干性的影响。

5.2 ScanSAR-Stripmap重复轨道差分干涉测量

我们将第4部分提出的关键技术应用到重复轨道差分干涉测量中，实验的总流程图如图3所示。然后将实验结果与常规条带式(Stripmap-Stripmap)差分干涉测量结果作对比。

实验的相干性图如图4(b)所示，通过与图4(c)对比可以看出，ScanSAR-Stripmap干涉的相干性明显低于Stripmap-Stripmap干涉的相干性，ScanSAR-Stripmap的平均相干性为0.49，而Stripmap-Stripmap的平均相干性为0.69，这是由于ScanSAR-Stripmap数据相隔时间比较长，数据之间的去相干更加严重，而且其中还有气候、季节等一些复杂因素影响相干性；第二，在将条带式数据处理成ScanSAR数据的时候，并不能保证两种数据片段之间的完全同步，这也会降低两种数据的相干性；第三，ScanSAR-Stripmap的分辨率更低，造成了相干性下降；最后，因为两种数据获取时的系统参数并不完全相同，这可能对相干性有一定影响。

实验的差分干涉图如图5所示，其中图5(a)是Bam地震的ScanSAR-Stripmap差分干涉图，图5(b)是Stripmap-Stripmap差分干涉图，粗略地看，(a)、(b)两种差分干涉图基本相同。我们再来定量地对比最后差分干涉测量得到的形变结果(图6)，ScanSAR-Stripmap结果的最大视线向形变量和最小视线向形变量分别为30.7 cm、−17.4 cm，Stripmap-Stripmap结果的最大视线向形变量和最小视线向形变量分别为30.5 cm、−17.3 cm，从图中也可以直观地看出两种结果是很吻合的。图(a)和(b)中的一些差别，主要是因为(a)的相干性较低，在解缠过程中掩膜掉了一些像元。可以以研究得比较成熟的常规Stripmap-Stripmap结果为正确结果，两种结果的如此符合证明

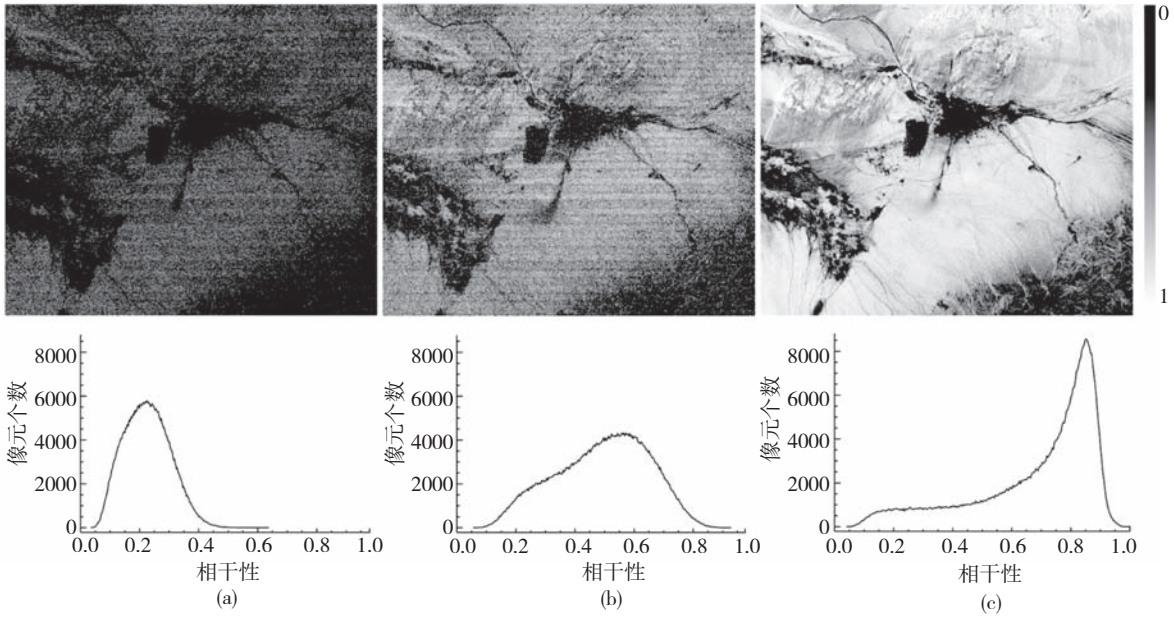

图4 相干性图及其直方图对比

(a) 未将条带式数据处理成ScanSAR数据时的ScanSAR-Stripmap相干性及其直方图；(b) 将条带式数据处理成ScanSAR数据时的ScanSAR-Stripmap相干性及其直方图；(c) Stripmap-Stripmap的相干性及其直方图

了ScanSAR-Stripmap干涉结果的正确性。

此外，ScanSAR数据分辨率较低，本实验中条带式数据的PRF又较小，所以条带式数据处理成ScanSAR数据之后，分辨率比ScanSAR数据的分别率还要低，造成ScanSAR-Stripmap干涉图的分辨率比真实ScanSAR数据之间干涉图的分辨率还低。

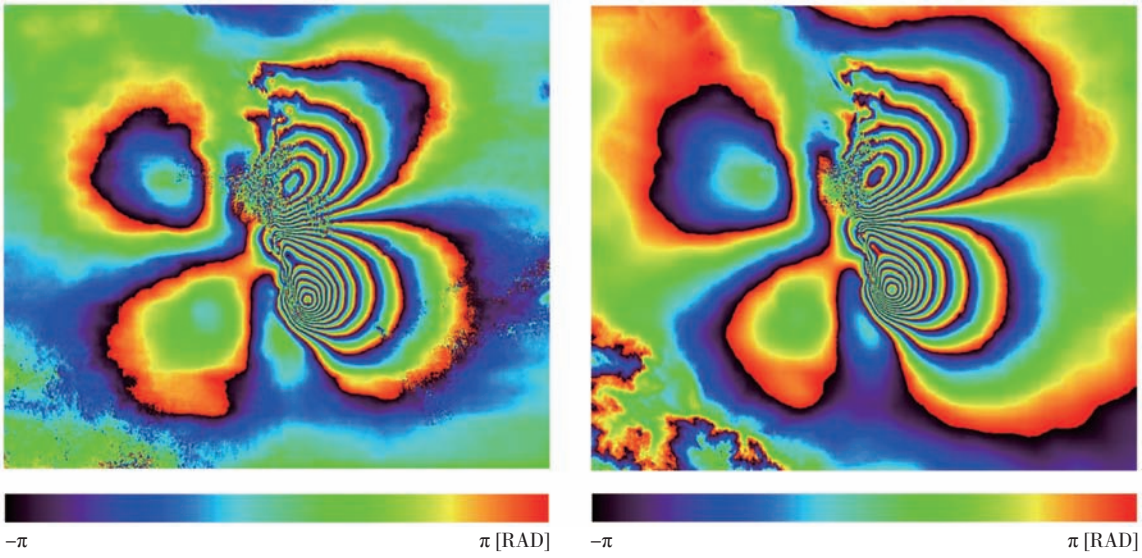

图5 ScanSAR-Stripmap与Stripmap-Stripmap差分干涉图比较(未解缠)

(a) ScanSAR-Stripmap；(b) Stripmap-Stripmap

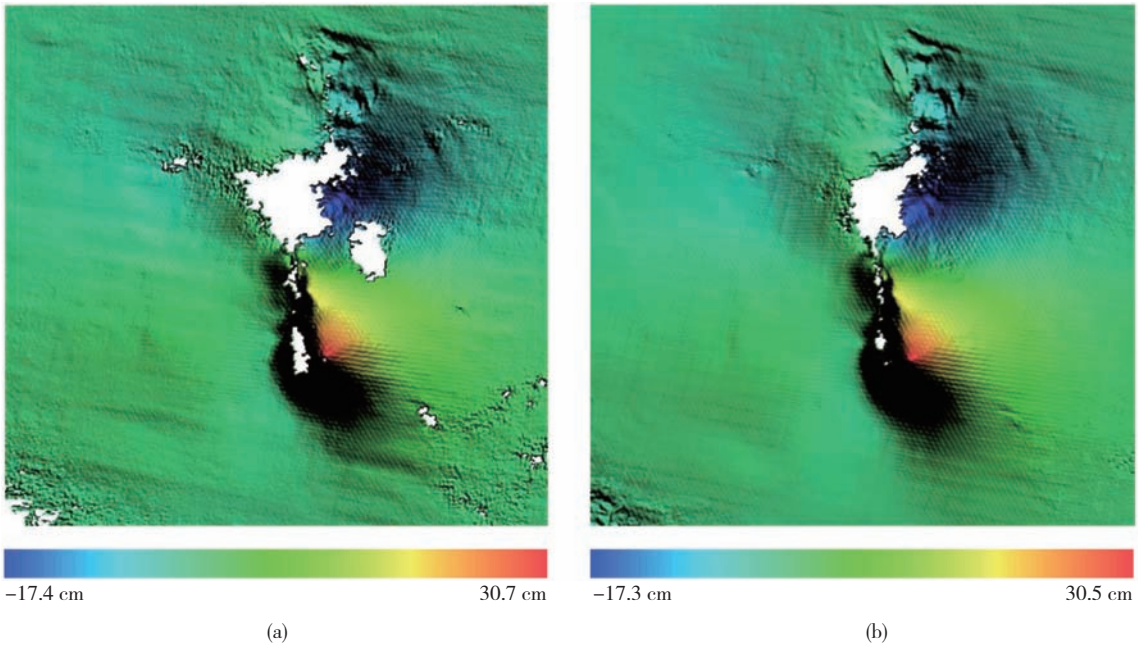

图6 两种差分干涉测量获取的巴姆地震形变量三维显示对比(白色区域为因相干性低而掩膜掉的区域)

(a) ScanSAR-Stripmap；(b) Stripmap-Stripmap

6 结 论

首先，针对ScanSAR-Stripmap干涉提出了一系列关键技术，包括两种模式数据PRF的统一、配准、不同步数据的去除等，并对条带式重复轨道干涉测量软件ROI_PAC进行了二次开发，利用Envisat ASAR WS和IM模式数据实现了伊朗巴姆地震ScanSAR-Stripmap差分干涉测量，并将获取的地表形变同常规

条带式数据获取的结果作了对比，发现测量结果非常符合，证明了本研究提出的技术的正确性。

其次，分析了ScanSAR-Stripmap干涉测量的相位组成，指出其特有相位项并通过实验验证了该相位项的存在。

最后，在研究过程中基于ROI_PAC开发了一套可用于ScanSAR-Stripmap干涉测量的程序。

志　谢　感谢JPL提供的免费干涉测量软件ROI_PAC。

REFERENCES

Bamler R, Geudtner D, Schattler B, Vachon P W, Steinbrecher U, Holzner J, Mittermayer J, Breit H and Moreira A. 1999. RADARSAT ScanSAR interferometry. IEEE International Geoscience and Remote Sensing Symposium Proceedings. Piscataway: Institute of Electrical and Electronics Engineers, Inc: 1517–1521

Cumming I G and Wong F H. 2005. Digital Processing of Synthetic Aperture Radar Data: Algorithms and Implementation. Norwood, MA: Artech House, Inc: 57–58, 144

Guarnieri A M, Cafforio C, Guccione P, Pasquali P and Desnos Y L. 2003a. ENVISAT ASAR ScanSAR interferometry. IEEE International Geoscience and Remote Sensing Symposium Proceedings. Piscataway: Institute of Electrical and Electronics Engineers, Inc: 1124–1126

Guarnieri A M, Guccione P, Pasquali P and Desnos Y L. 2003b. Multi-mode ENVISAT ASAR interferometry: techniques and preliminary results. *IEE Proceedings-Radar, Sonar and Navigation*, **150**(3): 193–200

Guccione P. 2006. Interferometry with ENVISAT wide swath ScanSAR data. *IEEE Geoscience and Remote Sensing Letters*, **3**(3): 377–381

Jia J Y. 2009. ScanSAR Interferometry Processing Techni-Que and Experiments. Beijing: Peking University: 79-80

JPL. [2009-09-17]. http://www2. jpl. nasa. gov/srtm/

Ortiz A B and Zebker H. 2007. ScanSAR-to-stripmap mode interferometry processing using ENVISAT/ASAR data. *IEEE Transactions on Geoscience and Remote Sensing*, **45**(11): 3468–3480

Rosen P A and Fielding E. 2009. ROI_PAC. OPEN CHANNEL FOUNDATION. [2009-09-18]. http: //www.openchannel software.com/projects/ROI_PAC

Rosen P A, Henley S, Peltzer G and Simons M. 2004. Updated repeat orbit interferometry package released. *EOS, Transactions American Geophysical Union*, **85**(5): 47

附中文参考文献

贾建瑛. 2009. ScanSAR干涉处理技术与实验研究. 北京：北京大学：79–80